Biogeosciences Discuss., https://doi.org/10.5194/bg-2018-276
Manuscript under review for journal Biogeosciences
Discussion started: 19 July 2018

Variation of Summer Oceanic pCO_2 and Carbon Sink in the Prydz Bay Using SOM Analysis Approach

Suqing Xu[1], Keyhong Park[2*], Yanmin Wang[3], Liqi Chen[1*], Di Qi[1], Bingrui Li[4]

1. Key Laboratory of Global Change and Marine-Atmospheric Chemistry, Third Institute of Oceanography, Xiamen 361005, PR China.
2. Division of Polar Ocean Sciences, Korea Polar Research Institute, Incheon 21990, South Korea.
3. Haikou Marine Environment Monitoring Central Station, State Oceanic Administration, Haikou 570100, China.
4. Polar Research Institute of China, Shanghai 200136, China.

Correspondence to: Liqi Chen (chenliqi@tio.org.cn);
Keyhong Park (keyhongpark@kopri.re.kr)

Abstract

This study applies a neural network technique to produce maps of oceanic surface pCO_2 in the Prydz Bay in the Southern Ocean on a 0.1 longitude · 0.1 latitude grid based on in-situ measurements during the 31th CHINARE cruise for February 2015. The study area was divided into three regions, Open-ocean region, Sea-ice region and Shelf region. The distribution of oceanic pCO_2 was mainly affected by physical process in the Open-ocean region where mixing and upwelling became the main controls. While in the Sea-ice region, oceanic pCO_2 changed sharply due to the strong change of seasonal ice. For the Shelf region, biological factor was the main control. The weekly oceanic pCO_2 was estimated using a self-organizing map (SOM) by four proxy parameters (Sea Surface Temperature, Chlorophyll a concentration, Mixed Layer Depth, and Sea Surface Salinity) to resolve the nonlinear relationships under complicated biogeochemical conditions in Prydz Bay region. The reconstructed oceanic pCO_2 coincides well with the in-situ investigated pCO_2 from SOCAT, in the root-mean-square error of 22.14 μatm. Prydz Bay was mainly a strong CO_2 sink in February 2015 with a monthly averaged uptake of 18.7±4.93 TgC. The oceanic CO_2 sink is pronounced in the Shelf region due to its lowest oceanic pCO_2 with peak biological production. Strong potential anthropogenic CO_2 uptake in the Shelf region will enhance the acidification in the deep water of Prydz Bay and affect the deep ocean acidification in the long run since it contributes to the formation of Antarctic bottom water.

Biogeosciences Discuss., https://doi.org/10.5194/bg-2018-276
Manuscript under review for journal Biogeosciences
Discussion started: 19 July 2018

30

31 1 Introduction

32 The role of the ocean south of 60°S in the transport of CO_2 to or from the atmosphere is still
33 uncertain despite of its importance of reducing anthropogenic CO_2 in the atmosphere (Sweeney
34 et al., 2000, 2002; Morrison et al., 2001; Sabine et al., 2004; Metzl et al., 2006; Takahashi et al.,
35 2012). This status derives from both the strong seasonal and spatial variations that occur around
36 Antarctica, and the difficulty of field measurements in the region for its hostile weather and
37 remoteness.

38 Following the Weddell and Ross seas, Prydz Bay, lying in the Indian Ocean section, is the
39 third largest embayment in the Antarctic continent. With Cape Darnley to the west and the
40 Zhongshan Station and Davis Station to the east, Prydz Bay is close to the Amery Ice Shelf to the
41 southwest and the West Ice Shelf to the northeast (Fig. 1). Water depth varies sharply northward
42 from 200 m to 3000 m.

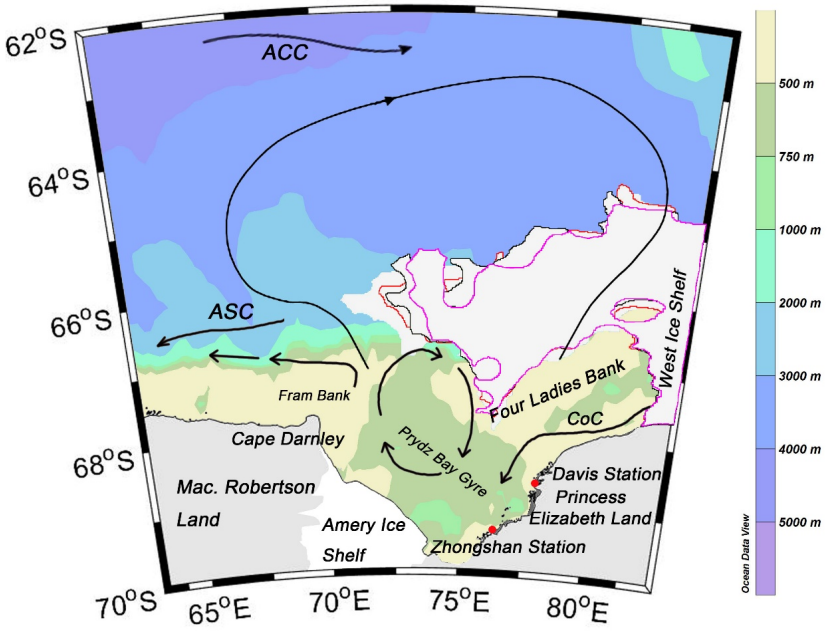

43

44 Fig. 1 The circulations in the Prydz Bay derived from Roden et al. (2013), Sun et al. (2013), Wu et al. (2017).
45 ASC: Antarctic Slope Current; CoC: Antarctic Coastal Current; ACC: Antarctic Circumpolar Current. The
46 weekly sea ice extents for our study periods were overlapped on the cruise. the pink line is for week-

1(20150202-20150209), the black line is for week-2 (20150210-20150217), the red line is for the week-3 (20150218-20150225) and the white shadow is for week-4 (20150226-20150305).

The inner continental shelf is dominated by the Amery Depression, which is mostly 600 to 700 m deep. The depression is bordered by two shallow banks (<200 m): Fram Bank and Four Ladies Bank, forming a spatial barrier to water exchange with the outer oceanic water (Smith and Trégure, 1994). The Antarctic Coastal Current (CoC) flows westward, bringing in cold waters from the east. When it reaches the shallow Fram Bank, it turns north and then part of it flows westward, while part of it turns eastward back to the inner shelf resulting in the clockwise rotating Prydz Gyre (see Fig.1). The circulation to the north of the bay is characterized by a large cyclonic gyre, extending from within the bay to the Antarctic Divergence at about 63°S (Nunes Vaz and Lennon, 1996; Middleton and Humphries, 1989; Smith et al., 1984; Roden et al., 2013; Wu et al., 2017). The inflow of this large gyre hugs the eastern rim of the bay, and favors the onshore intrusions of warmer modified Circumpolar Deep Water (mCDW) across the continental shelf break (Heil et al., 1996). A westward flow along the shelf, that is part of the wind-driven Antarctic Slope Current (ASC), supplies water to Prydz Bay. In the austral summer, with longer daylight and increased solar radiation, sea surface temperature increases, ice shelf breaks and sea ice melts, resulting in stratification of the water column. Prydz Bay region is host to a marine ecosystem that interacts with the physical environment which makes it complicated to study the spatiotemporal variability and mechanism of oceanic pCO_2.

Despite the importance of carbon cycle in the Southern Ocean, the observations are rather limited to analyze the spatiotemporal variation in the Prydz Bay. The analysis of temporal variability and the spatial distribution mechanism of oceanic pCO_2 in Prydz Bay was limited to cruises or stations (Gibsonab and Trullb, 1999; Gao et al., 2008; Roden et al., 2013). To estimate regional sea-air CO_2 fluxes, it is necessary to interpolate between in-situ measurements to obtain the maps of oceanic pCO_2. Such an interpolation approach, however, is still a difficult task because observations are too sparse in both time and space to capture the high pCO_2 variability. Satellites do not measure pCO_2 but they give access to parameters related to the processes that control its variability. The seasonal and geographical variability of surface water pCO_2 is indeed much greater than that of atmospheric pCO_2. Therefore, the direction of the sea-air CO_2 transfer is mainly regulated by the oceanic pCO_2. Linear regression extrapolation method has been

Biogeosciences Discuss., https://doi.org/10.5194/bg-2018-276
Manuscript under review for journal Biogeosciences
Discussion started: 19 July 2018

applied to expand the cruise data to a big scale area to study the carbon cycle in the Southern Ocean (Rangama et al., 2005; Chen et al., 2011; Xu et al., 2016), however, the linear regression relied simply either on chlorophyll-a (CHL) or on sea surface temperature (SST) parameter. Thus, this method is insufficient to represent all the controlling factors. In this study, we applied self-organizing map (SOM) analysis to expand our observed data sets and estimated the oceanic pCO_2 in the Prydz Bay during the February 2015.

The SOM analysis, based on neural network (NN), a type of artificial neural network, has been proved to be a useful method for extracting and classifying features in geoscience (Gibson et al., 2017; Huang et al., 2017b). In oceanography, SOM has been applied for the analysis of various properties of the seawater such as sea surface temperature (Iskandar, 2010; Liu et al., 2006), chlorophyll concentration (Huang et al., 2017a; Silulwane et al., 2001). In the past decade, SOM has also been applied to produce basin-scale pCO_2 maps mainly in the North Atlantic and Pacific Ocean by using different proxy parameters (Lafevre et al., 2005; Friedrich & Oschlies, 2009a, 2009b; Nakaoka et al., 2013; Telszewski et al., 2009; Hales et al., 2012; Zeng et al., 2015; Laruelle et al., 2017). SOM has been proved to be useful to expand a spatial-temporal coverage of direct measurements or to estimate properties whose satellite observations are technically limited. One of the main benefits of the neural network method over the more traditional techniques is that there is more accurate representation of the highly variable system of interconnected water properties (Nakaoka et al., 2013).

During the 31th CHINARE in Prydz Bay, we have conducted a survey on partial pressure of CO_2 in oceanic water and atmosphere from the beginning of February to the early of March (data of the cruise track is shown in Fig. 2). This study is aimed to apply the SOM method to reconstruct the temporal and spatial variability of oceanic pCO_2 distribution in Prydz Bay from 63°E to 83°E, 64°S to 70°S and discuss the capability of carbon absorption in February 2015.

The paper is organized as followed. Section 2 provides the descriptions of the in-situ measurements and the SOM methods. Section 3 presents the analysis and discussion of the results. Section 4 presents the summary.

2 Data and method

2.1 in situ data

The in situ underway pCO_2 of marine water and atmosphere was collected during the 31th CHINARE when R/V Xuelong sailed from east to west at the beginning of February 2015 (see

Fig.2-a, b). Sea water at 5 meters underneath the sea surface was pumped continuously to the GO system (GO Flowing pCO_2 system, General Oceanics Inc., Miami FL, USA), and the partial pressure of the sea surface water is measured by an infrared analyzer (LICOR, USA, Model 7000). The analyzer was calibrated every 2.5-3 h using four standard gases at pressures of 88.82 ppm，188.36 ppm，399.47 ppm，528.92 ppm supplied by NOAA's Global Monitoring Division. The accuracy of the measured pCO_2 is within 2 μatm (Pierrot et al., 2009). The underway pCO_2 in atmosphere was simultaneously collected by the GO system.

Sea ice melt has a significant impact on the local stratification and circulation in polar region. Salinity records the physical processes. During freezing, salt is excluded from ice, and thus increase the ocean surface salinity. This is so called brine rejection. When ice begins to melt, fresher water is added into the ocean to dilute the ocean water, i.e., reducing the salinity. In this study, we treat salinity as an index for the change of sea ice. The underway sea surface temperature SST and conductivity was recorded by a Conductivity-Temperature-Depth sensor (CTD, Seabird SBE 21) along the cruise track. Later sea surface salinity was calculated according to the recorded conductivity and temperature. The distributions of underway SST and SSS were shown in Fig.2 c and d.

In previous studies it has been reported that the summer sink in Prydz Bay is clearly biologically driven and the pCO_2 change is often well-correlated with surface chlorophyll-a concentration (Rubin et al., 1998; Gibsonab et al., 1999). When sea ice starts to melt, the active biological process affects oceanic pCO_2 significantly (Chen et al., 2011; Xu et al., 2016). The chlorophyll-a value is regarded as an important controlling factor of pCO_2. Daily Modis chlorophyll-a data of 4 km resolution (http://oceancolor.gsfc.nasa.gov) are interpolated to the observation section and time. The interpolated result along the cruise track is shown in Fig.2e.

The ocean mixed layer is characterized as having nearly uniform physical properties throughout the layer with a gradient in properties at the bottom of the layer. The mixed layer links the atmosphere to the deep ocean and plays a critical role in climate variability. Very few studies have emphasized the importance of accounting for the vertical mixing through the mixed layer depth (MLD, Dandonneau, 1995; Lüger et al., 2004). The stability and stratification prevent the upward mixing of nutrients and limits the biological production and thus affect sea-air CO_2 exchange. The vertical profile of sea water including potential density was measured by a Seabird SBE 11. Comparison of MLD based on the difference and gradient criteria (Brainerd

Biogeosciences Discuss., https://doi.org/10.5194/bg-2018-276
Manuscript under review for journal Biogeosciences
Discussion started: 19 July 2018

and Gregg, 1995; Thomson and Fine, 2003) suggested that MLD determined using a difference criterion is more stable in the Southern Ocean. Following Dong et al. (2008), we calculated the mixed layer depth (see Fig.2-f) based the difference criteria, of with sigma theta changed by 0.03 kg/m^3. The MLD value at stations were later gridded linearly to match the spatial and temporal resolution of the in situ data along the cruise track.

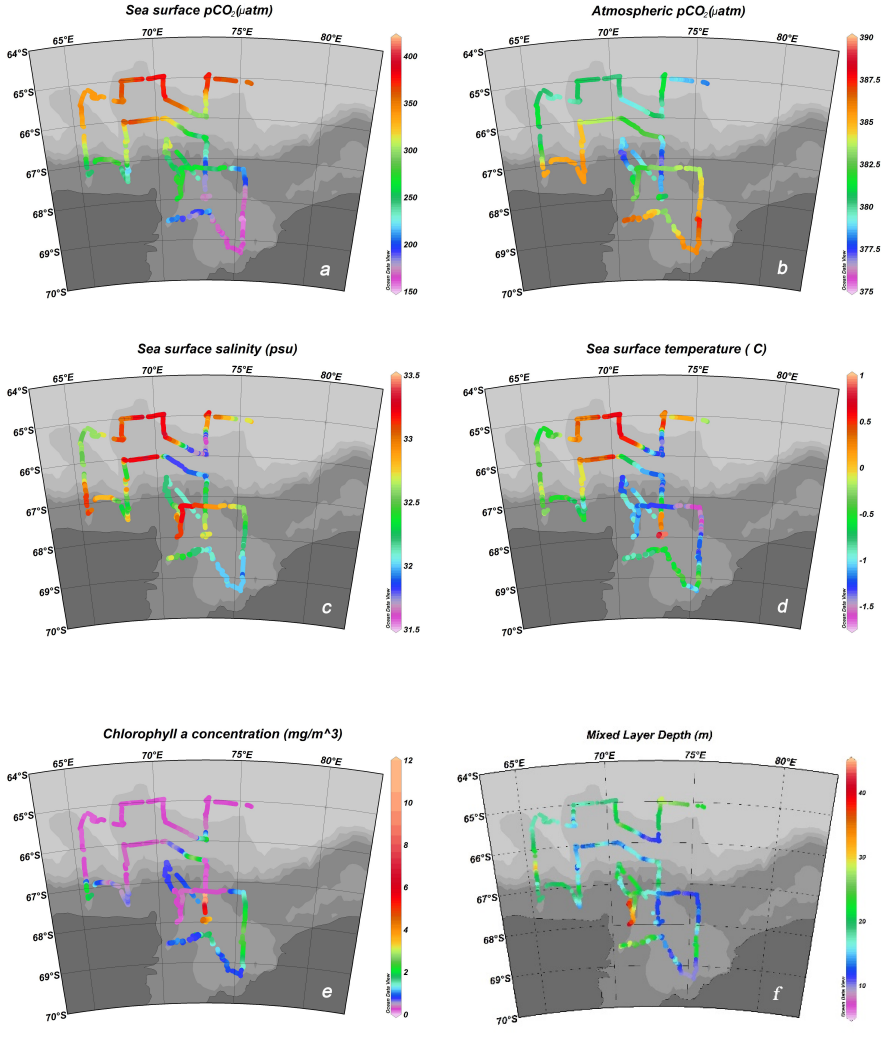

Fig.2 the distributions of underway oceanic and atmospheric pCO_2, SST, SSS, and CHL gridded from MODIS, and MLD gridded from sta · surveys.

Biogeosciences Discuss., https://doi.org/10.5194/bg-2018-276
Manuscript under review for journal Biogeosciences
Discussion started: 19 July 2018

2.2 SOM method and input variables

We hypothesize that oceanic pCO_2 can be reconstructed through the SOM based multiple non-linear regression with four proxy parameters (Eq. 1): sea surface temperature (SST), the abundance of photo-synthesizing organisms in the surface ocean represented by the chlorophyll-a concentration (CHL), mixed layer depth (MLD), and sea surface salinity (SSS).

$$pCO_2^{sea}=\text{SOM (SST, CHL, MLD, SSS)} \quad (1)$$

The SOM is trained using unsupervised learning to project the input space of training samples to a feature space (Kohonen, 1984), which is usually represented by grid points in two-dimension space. Each grid point, also called neuron cell, is associated with a weight vector having the same number of components as the vector of input data (Zeng et al., 2017). During the SOM analysis three steps are taken to estimate oceanic pCO_2 fields (see Fig. 3). Input variables to estimate pCO_2 are prepared in a vector form. The SOM analysis was carried out by the MATLAB SOM tool box 2.0 (Vesanto, 2002). It has been developed by the Laboratory of Computer and Information Science in the Helsinki University of Technology and is available from the following web page: http://www.cis.hut.fi/projects/somtoolbox.

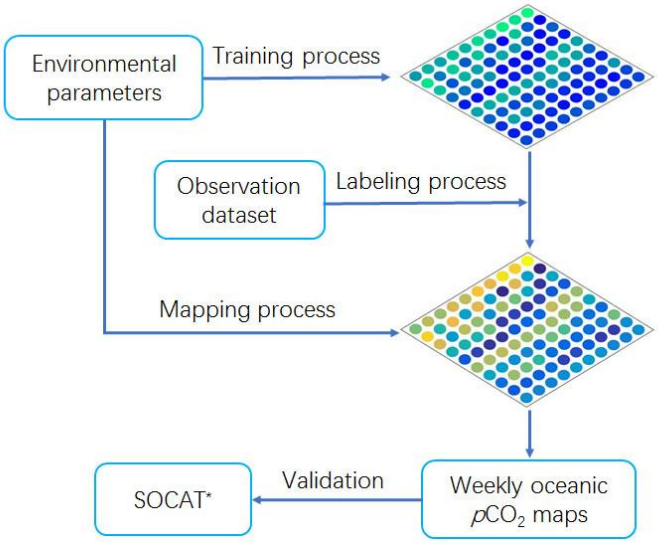

Fig. 3. Schematic scheme of the main three step involved in the SOM neural network calculations leading to weekly pCO_2 maps for February 2015.

More realistic pCO_2 estimates were expected from the SOM analysis when the distribution and variation range of the labeling variables closely reflect the training data sets (Nakaoka et al.,

Biogeosciences Discuss., https://doi.org/10.5194/bg-2018-276
Manuscript under review for journal Biogeosciences
Discussion started: 19 July 2018

2013) while our underway measurements with pCO_2 value have a spatiotemporal limitation to cover the range of the variation of training data sets. Before the training process, the input training dataset and labeling dataset are analyzed and prospectively normalized to make an even distribution. The statistics and range of the values of each variable are presented in Table1. When the dataset of four proxy parameters were logarithmically normalized the skewness of CHL and MLD changed obviously especially for the training dataset. The *N* coverage represents the percentage of the training data that are labeled. The data *N* coverage of training data set of CHL, MLD and SSS are 82.1%, 85% and 81.1% respectively, which might be due to the insufficient spatiotemporal coverage and or bias between the labeling and training data sets. The *N* coverage of the logarithmically datasets changed to 93.6% and to 98.7% respectively for CHL and MLD. Thus the common logarithm of CHL and MLD values are used for both the training and labeling datasets in order to resolve the data coverage issue from significantly increasing the data coverage as well as to overcome the weighting issue raised from the different magnitude among the variables (Ultsch and Röske, 2002).

Table 1. Statistics of labeling and training data sets showing the distribution and coverage of each variable.

Coverage of each variable		SST(C)	CHL(mg/m^3)	MLD(m)	SSS(psu)
Labeling	Max	0.81	11.13	40.69	33.81
	Min	-1.44	0.17	7.84	32.43
	Mean	-0.27	3.80	14.41	33.27
	Skewness	0.4(-0.2)$^{\#}$	0.8(-0.3)	0.9(0.4)	0.6(0.6)
Training	Max	2.48	40.17	48.95	34.17
	Min	-1.8	0.06	10.46	28.64
	Mean	-0.53	1.36	14.79	33.16
	Skewness	0.5(-0.6)	4.3(0.5)	2.6(0.8)	-0.9(-1.0)
	N coverage* (%)	91.3(92.5)$^{+}$	82.1(93.6)	85.0(98.7)	81.1(80.4)

the skewness of common logarithm of each variable is shown in the parenthesis.

* [number of training data within the labeling data range]/[total number of training data]

+ the percent labeling data coverage of normalized variables is shown in the parenthesis

During the training process, a neuron's weight vectors are repeatedly trained by being presented with the input vectors, until the neural network sufficiently represents the nonlinear interdependence of proxy parameters used in training. This process results in clustering of similar neurons and self-organization of the map. The observed oceanic pCO_2 is not needed at the first step.

Biogeosciences Discuss., https://doi.org/10.5194/bg-2018-276
Manuscript under review for journal Biogeosciences
Discussion started: 19 July 2018

During the second process, each preconditioned SOM neurons is labeled with an observed oceanic pCO_2 value. The labeling dataset consisting of the observed pCO_2 and the normalized SST, CHL, MLD and SSS is presented to the neural network and then a winner neuron is found. After the labeling process, neurons are represented by five-dimensional vectors.

Finally, during the mapping process, the labeled SOM neurons created by the second process and trained SOM neurons created by the first process are used to produce oceanic pCO_2 of the winner neuron according to the geographical grid points of the study area.

We used four datasets including SST, CHL, MLD, and SSS **(SCMS)** to train the SOM. For SST, we used daily data from AVHRR ONLY (https://www.ncdc.noaa.gov/oisst) of 1/4° spatial resolution (see Fig.S1). CHL data are the 8-D composite chlorophyll-a data from MODIS-Aqua (http://oceancolor.gsfc.nasa.gov) at a space resolution of 4km (see Fig.S2). We also used the daily SSS and MLD data (see Fig.S3-4) from the 1/12° global analysis and forecast product from the Copernicus Marine Environment Monitoring Service (CMEMS, http://marine.copernicus.eu/). Sea ice concentration is from the daily 3.125-km AMSR2 dataset (Spreen et al., 2008, available on https://seaice.uni-bremen.de, see Fig.S5).

All the daily datasets were first averaged to be 8-d fields regarded as weekly for this study. From the beginning of February to the early of March we have four independent week series, which are week-1 (from 02/02/2015 to 02/09/2015), week-2 (from 02/10/2015 to 02/17/2015), week-3 (from 02/18/2015 to 02/25/2015), and week-4 (from 02/26/2015 to 03/05/2015). The weekly proxy parameters (**SCMS**) were further re-gridded with a horizontal resolution of 0.1° · 0.1°. In the SOM analyses, input vectors with missing elements are excluded. Consequently, oceanic pCO_2 created in this study has weekly frequency and 0.1 longitude · 0.1 latitude resolution from 63°E to 83°E and 64°S to 70°S.

We compared the assimilated datasets of SST from AVHRR with in situ measurements obtained by CTD along the cruise. The relationship is 0.97 and the root-mean-square error (RMSE) is 0.2°C. The SSS and MLD fields from the Global Forecast system compare reasonably well with the in situ measurements, with relationships of 0.76 and 0.74, respectively and the RMSE of 0.41 and 5.15m. The uncertainty of the Modis CHL data in the Southern Ocean is about 35% (Xu et al., 2016). For the labeling procedure, the observed oceanic pCO_2 together with corresponding in situ SST, SSS, MLD, and Modis CHL product in vector form are used as the input dataset.

Biogeosciences Discuss., https://doi.org/10.5194/bg-2018-276
Manuscript under review for journal Biogeosciences
Discussion started: 19 July 2018

2.3 Validation of SOM derived oceanic pCO_2

To validate the oceanic pCO_2 reconstructed by the SOM analysis, we used the fugacity of oceanic CO_2 datasets (referred as "SOCAT" data hereinafter) from the Surface Ocean CO_2 Atlas (SOCAT: http://www.socat.info) version 5 database (Bakker et al., 2016). In Pacific Ocean, the Atlantic Ocean or regions away from coast, datasets from different years can be assimilated to a reference year to have a good spatial coverage according to the equilibrium between sea surface and atmosphere (Takahashi et al., 2006; Wong et al., 2010; Nakaoka et al., 2013). However, the same approach should be applied carefully because the sea ice condition varies from year to year in the Southern Ocean. The sea ice cover has a great impact on the oceanic pCO_2. SOCAT data in February from different years do have a good spatial coverage in Prydz Bay. However we could only select dataset for our study period in 2015 (see Fig. 4-a) although it covers limited area in study region. We recalculated pCO_2 values from the obtained fCO_2 offered in SOCAT data according to the fugacity correction (Pfeil et al., 2013).

2.4 Carbon uptake in the Prydz Bay

The flux of CO_2 between the atmosphere and the ocean was determined by two items. One is the difference in CO_2 concentration across the sea-air interface and the other is the transfer velocity which is a function primarily of wind speed and temperature. The equation to calculate the sea-air carbon flux was simplified as a function of wind speed and delta pCO_2 (from sea to air) in eq. 2, Xu et al. (2016). For the weekly estimation in this study, the scaling factor for the gas transfer rate is changed to 0.251 for a shorter time scale and at intermediate wind speed ranges (Wanninkhof, 2014). For each grid, weekly sea-air carbon flux in the Prydz Bay can be estimated by Eq. (2):

$$Flux_{sea\text{-}air}(\text{g C/(m}^2 \cdot\text{week)}) = 30.8\times10^{-4}\times U^2\times (pCO_2^{sea} - pCO_2^{air}) \quad (2)$$

where U represents wind speed 10 m above sea level, pCO_2_sea and pCO_2_air are partial pressure of CO_2 in sea water and atmosphere.

We downloaded weekly ASCAT wind speed data (http://www.remss.com/, see Fig. S6) of 1/4 degree and then regridded the dataset to fit the 0.1 longitude · 0.1 latitude spatial resolution of SOM derived oceanic pCO_2. We regridded the atmospheric pCO_2 collected along the cruise track to fit the spatial resolution of SOM derived oceanic pCO_2 by linear method. The total carbon uptake was then obtained by accumulating the flux of each grid by each area according to Jiang et al. (2008) and with the proportion of ice-free area (Xu et al., 2016).

Biogeosciences Discuss., https://doi.org/10.5194/bg-2018-276
Manuscript under review for journal Biogeosciences
Discussion started: 19 July 2018

260

2613 Results and discussion

2623.1 the distributions of underway measurements

263 From the beginning of February, R/V Xuelong sailed from east to west along the sea ice
264edge. Based on the water depth and the sea ice condition, the study area is robustly divided into
265three sectors, the Open-ocean region, Sea-ice region and the Shelf region.

266 The Open-ocean region was from 66°S northward to 64°S where locates the Antarctic
267Divergence Zone and with water depth greater than 3000 m. The AD zone was characterized by
268high nutrients and low chlorophyll (HNLC) concentrations with high pCO_2 attributed to
269upwelling of deep waters, suggesting the importance of physical processes (Burkill et al., 1995;
270Edwards et al., 2004). Underway sea surface temperature in this region are relatively high with
271an average value of 0.36°C due to the upwelling Circumpolar Deep Water (CDW) while in the
272sea ice edge (73°E, 65.5°S to 72°E, 65.8°S) SST decreased below -1°C. From 67.5°E westward,
273affected by the large gyre, cold water from the high latitude lowered down SST to below 0°C.
274Near the sea ice edge, SSS decreased quickly to 31.7 due to the diluted water, while along the
27565°S cruise it reached to 33.3, and then western from 67.5°E affected by the fresher and colder
276water brought by the large gyre it decreased to 32.5. The satellite chlorophyll-a image showed
277that it was of low value of 0.45 mg/m^3 except when the vessel near the sea ice edge CHL
278increased to be 2.26 mg/m^3. The distribution of MLD varied along the cruise. Near the sea ice
279edge, because of the melting of ice and direct solar warming, it constituted a low-density cap
280over the water column the MLD was as shallow as 10.21 m. The maximum value of MLD in
281Open-ocean region is 31.67 m. In the Open-ocean region atmospheric pCO_2 was stable from
282374.6 µatm to 387.8 µatm. Oceanic pCO_2 varied from 291.98 µatm to 379.31 µatm with an
283average value of 341.48 µatm. Along the 65°E cruise in the east part of the Open-ocean region,
284oceanic pCO_2 was relative high reaching an equilibrium with atmospheric pCO_2. The lowest
285value was found near the sea ice edge due to biological consume. For the western part, oceanic
286pCO_2 decreased a little due to the mixture of low pCO_2 from higher latitude by the large gyre.
287Mixing and upwelling were the dominant factors for oceanic pCO_2 in this region.

288 The seasonal Sea-ice region (from 66°S to 67.25°S) is between the Open-ocean region and
289the Shelf region. In this sector, sea ice changed strongly and water depth varied sharply from 700
290m to 2000 m. Sea ice kept changing and reforming from the late of February to the beginning of

21
22

Biogeosciences Discuss., https://doi.org/10.5194/bg-2018-276
Manuscript under review for journal Biogeosciences
Discussion started: 19 July 2018

March. Sea surface temperature decreased slightly compared to that in the Open-ocean region and the average value was -0.72°C. With the rapid sea ice changing, sea surface temperature and salinity varied sharply from -1.3°C to 0.5°C and from 31.8 to 33.3 respectively. When sea ice melted, water temperature increased, biological activities became active and chlorophyll-a value increased by a small amount to an average of 0.51 mg/m^3. Due to the rapid change of sea ice cover, the value of MLD varied from 12.8 m to 30.9 m. The average value of oceanic pCO_2 was 276.48 µatm ranging from 190.46 µatm to 364.43 µatm.

The Shelf region (from 67.25°S southward) is characterized of low depth below 700m, surrounding by the Amery Ice Shelf, West Ice Shelf, and the stretching permanent sea ice from the West Ice Shelf, formed by modification of low temperature and salinity shelf water (Smith et al., 1984). Two shallow banks (<200m): Fram Bank to the north-west and Four Ladies Bank to the north-east, forming a spatial barrier for the inner shelf to water exchange with the outer oceanic water (Smith and Tréguer, 1994). Prydz Bay coastal current flowed from east to west in the semi-close bay. There is always a fresher, warmer surface layer over the bay which is known as the Antarctic Surface Water (ASW). During our study period, the Shelf region was completely ice free, a large volume of freshwater was released into the bay, resulting in low sea surface temperature (an average of -0.61°C) and salinity (an average is 32.4). As shown in Fig.2-f, the mixed layer depth is low in most of the inner shelf. Due to the vast shrink of sea ice and strong stratification in the upper water, algal bloomed and chlorophyll value was high with an average of 1.93 mg/m^3. The oceanic pCO_2 in this region turned out to be the lowest in three sectors. The average of oceanic pCO_2 is 198.72 µatm with a range from 151.70 µatm to 277.78 µatm. Chlorophyll-a value shows remarkably as high as 11.04 mg/m^3 from 72.3°E, 67.3°S to 72.7°E, 68°S when sea ice retreated eastwardly. In the bay mouth close to the Fram Bank, due to the local upwelling water salinity increased remarkably to around 33.2. Biological pump becomes the dominant factor of the distribution of oceanic pCO_2.

3.2 Quality and maps of SOM derived oceanic pCO_2

We selected SOM derived oceanic pCO_2 to fit the cruise track of SOCAT for a same period using a nearest grid method. The slope of the scatter plot showed that SOM derived oceanic pCO_2 is lower than the SOCAT data (see Fig. 4-b). The RMSE between the SOCAT data and SOM derived result is calculated as follows:

Biogeosciences Discuss., https://doi.org/10.5194/bg-2018-276
Manuscript under review for journal Biogeosciences
Discussion started: 19 July 2018

$$RMSE=\sqrt{\frac{\sum\left(pCO_2^{sea}(SOM)-pCO_2^{sea}(SOCAT)\right)^2}{n}} \quad (3)$$

where n is the number of the validation dataset. The RMSE could be used interpreted as an estimation of the uncertainty in SOM derived oceanic pCO_2 in Prydz Bay. In this study, the RMSE is 22.14 µatm. This is consistent with the accuracy (6.9 µatm to 24.9 µatm) achieved in previous studies using neuron methods to reconstruct oceanic pCO_2 (Nakaoka et al., 2013, Zeng et al., 2002; Sarma et al., 2006; Jo Y H et al., 2012; Hales et al., 2012; Telszewshi M., et al., 2009). However, this precision of this study is not as good as most of the neuron methods. Increasing the spatial coverage of the labeling data will help to increase the precision of SOM derived oceanic pCO_2.

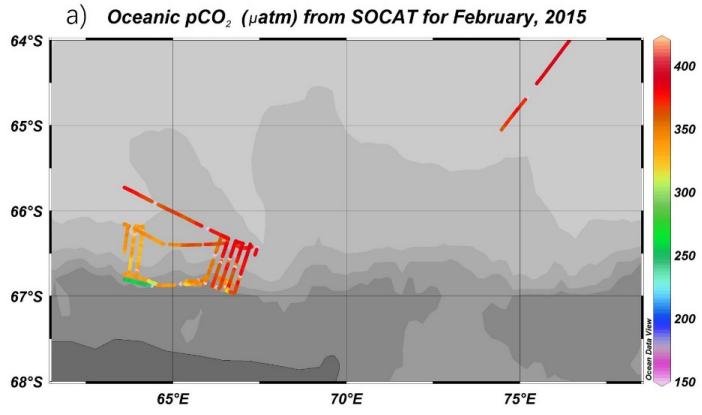

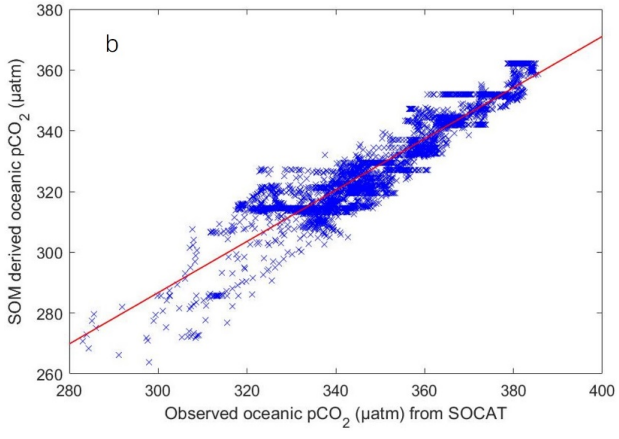

Biogeosciences Discuss., https://doi.org/10.5194/bg-2018-276
Manuscript under review for journal Biogeosciences
Discussion started: 19 July 2018

Fig. 4 a)The cruise lines from SOCAT to validate the SOM derived oceanic pCO_2 for the study period in 2015;
b) Comparison between the SOM derived and observed SOCAT oceanic pCO_2.

3.3 Spatial and temporal distributions of SOM derived oceanic pCO_2

In austral winter, the entire Prydz Bay basin is fully covered by sea ice except for a few areas, the polynyas, remaining open due to katabatic winds (Liu et al., 2017). As the austral summer starts, with the increasing sunlight, sea surface temperature increased, ice shelf broke and drifted out. Due to coincident high wind speeds, monthly peak tides, and/or the effect of penetrating ocean swell, sea ice in the Shelf region started to melt in early summer (Lei et al., 2010), forming Prydz Bay Polynya. The AMSR2 sea ice extent and mean ice concentration in each region are shown in Fig. 5, respectively. The Shelf region has the least sea ice extent ($1.38 \times 10^4 km^2$) and concentration (13.54%), without significant temporal variation. The semi-close polynya functions as a barrier for water exchange in the Shelf region and lack of significant bottom-water production, hindering outflow of continental shelf water and inflow of Antarctica circle deep water, resulting in a longer residence time for the vast melting water and enhanced stratification (Sun et al., 2013). Due to vast sea ice melting, sea surface salinity decreased, algae bloomed, the biological productivity increase promptly, the value of chlorophyll-a concentration reached the peak, the Shelf region became a strong CO_2 sink. As shown in Fig. 6, an obvious drawdown of oceanic pCO_2 in Shelf region due to phytoplankton photosynthesis during the summer bloom. The lowest oceanic pCO_2 in the Shelf region was 153.83 µatm except in the edge of West Ice Shelf oceanic pCO_2 reached over 300 µatm. The oceanic pCO_2 was the lowest in week-1 (from 02/02/2015 to 02/09/2015) which is coincident with a peak/bloom in the chlorophyll-a evidenced by the satellite images.

Biogeosciences Discuss., https://doi.org/10.5194/bg-2018-276
Manuscript under review for journal Biogeosciences
Discussion started: 19 July 2018

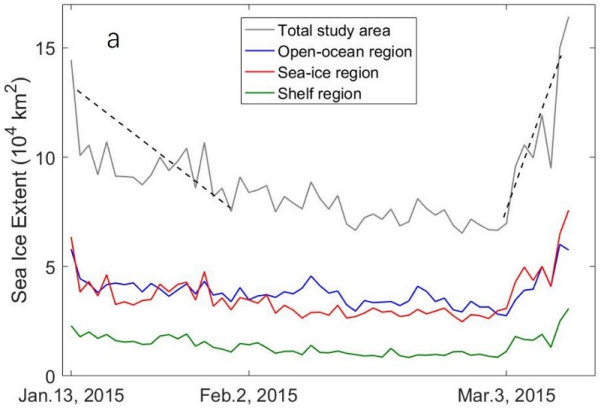

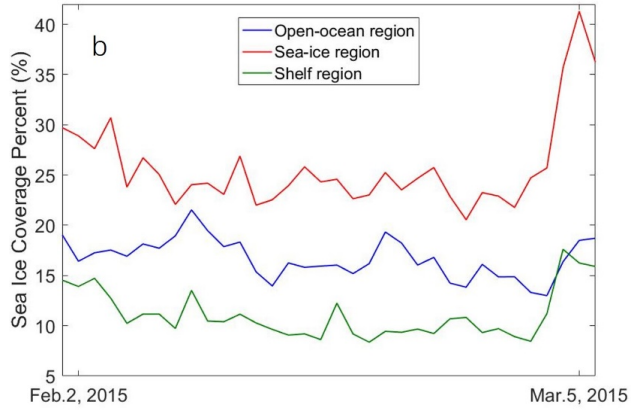

Fig. 5 a) Sea ice extent (unit: 10^4 km^2) in study area (gray line) and three sub-regions (blue: Open-ocean region; red: Sea-ice region; green: Shelf region); b) Averaged ice concentration in three sub regions from Feb. 2, 2015 to Mar. 5, 2015.

As shown in Fig.5-a, Sea ice in Open-ocean region and Sea-ice region started to melt from Jan 13, 2015, during February it decreased to the lowest and then it began to reform from Mar.3, 2015. The average sea ice extent in Open-ocean region and Sea-ice region were $3.85 \cdot 10^4$ km^2 and $3.56 \cdot 10^4$ km^2. During our study period, in the Sea-ice region, sea ice kept melting and reforming rapidly and the average value of sea ice coverage percent is 29.54%. Oceanic pCO_2 changed sharply from 155.86 µatm to 365.11 µatm.

In the Open-ocean region, sea ice started to melt in the beginning of February. In most area of the Open-ocean region it was sea ice free while the average sea ice coverage is only 18.14%.

Biogeosciences Discuss., https://doi.org/10.5194/bg-2018-276
Manuscript under review for journal Biogeosciences
Discussion started: 19 July 2018

370The ice cover is mainly associated with the outstretching permanent sea ice. Affected by the
371upwelling CDW, the stability of water was weak and not suitable for the growth of
372phytoplankton. It is also evidence by, the observed biological productivity, which was below 0.5
373mg/m^3. From the distribution of SOM derived oceanic pCO_2 as shown in Fig. 6, oceanic pCO_2
374value was the highest compared to the Sea-ice region and the Shelf region. From week-1 to
375week-4, oceanic pCO_2 increased a little and reached 381.42 µatm which was equivalent to that of
376atmosphere. In the western part of Open-ocean region, oceanic pCO_2 decreased due to mixing
377with low oceanic pCO_2 flew from the high latitude by the large gyre.

378

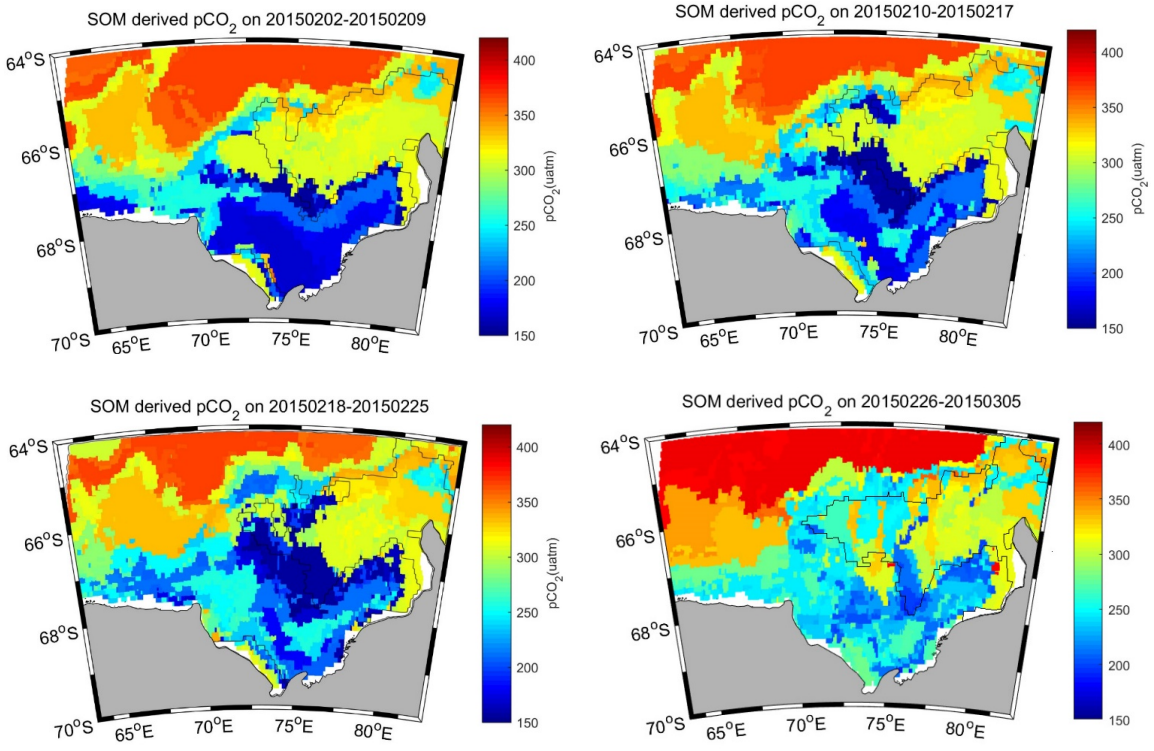

379 Fig. 6 Weekly SOM derived Prydz Bay pCO_2 (unit: µatm) distribution in February 2015, the black
380contour representing sea ice concentration of 15%.

3813.4 **Carbon uptake in Prydz Bay**

31
32

Biogeosciences Discuss., https://doi.org/10.5194/bg-2018-276
Manuscript under review for journal Biogeosciences
Discussion started: 19 July 2018

382 Over the whole study period, the averaged ocean-air pCO_2 difference ($\triangle pCO_2$) is largest
383 in the Shelf region, then follows the Sea-ice region and Open-ocean region. $\triangle pCO_2$ from Shelf
384 region changed from -184.31µatm to -141.00 µatm as the chlorophyll decreased. The sea-air
385 difference of pCO_2 in the Sea-ice region and Open-ocean region showed the same pattern. It
386 increased from week1 to week3 then decreased in week4. Based on the $\triangle pCO_2$ and wind speed,
387 the uptake of CO_2 (eq. 2) in three regions is presented in Fig. 7. In Shelf region the low oceanic
388 pCO_2 levels drove relatively intensive CO_2 uptake from the atmosphere. Carbon uptake in Shelf
389 region increased from week-1 (2.13 TgC) to week-2 (2.24 TgC) due to increased wind speed.
390 While in week-3, wind speed slowed down, resulting in the uptake of CO_2 in Shelf region
391 decreased to 1.70 TgC. In week-4, even the $\triangle pCO_2$ was the lowest, the total absorption still
392 increased to be 2.03 TgC due to the high wind speed (averaged value of 7.9 m/s).

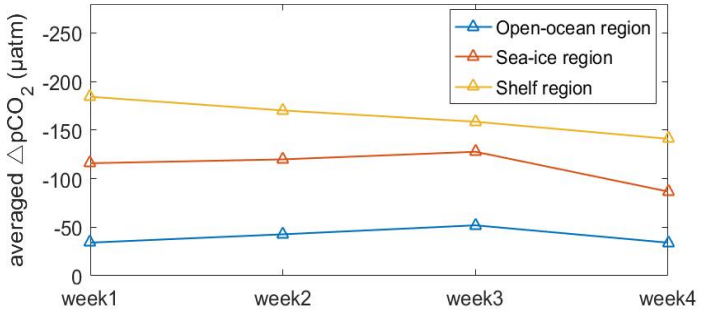

393

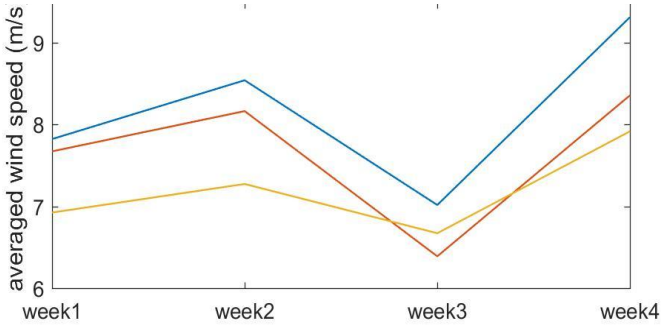

394

33
34

Biogeosciences Discuss., https://doi.org/10.5194/bg-2018-276
Manuscript under review for journal Biogeosciences
Discussion started: 19 July 2018

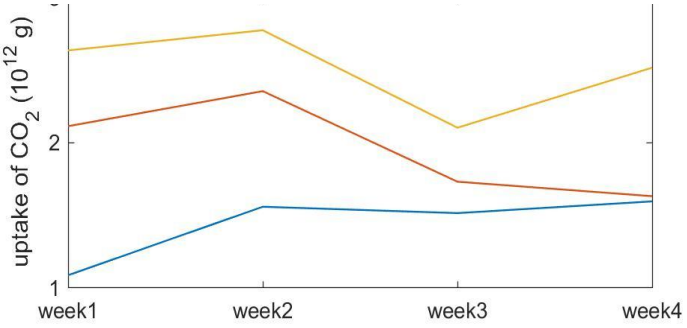

395

396 Fig. 7 Timeseries of weekly averaged $\triangle pCO_2$, wind speed and uptake of atmospheric CO_2 in Open-ocean
397 region (blue line, the negative value means the direction from sea to air), Sea-ice region (red line) and Shelf
398 region (yellow line).

399

400 Studies have reported that Prydz Bay is a strong carbon sink in the austral summer. Roden et
401 al. (2013) estimated the coastal Prydz Bay to be an annual net sink for CO_2 of 0.54±0.11 mol/
402 (m^2·year), i.e., 1.48±0.3 g/(m^2·week). Gibsonab et al. (1999) estimated the averaged summer ice-
403 free period sea-air flux to be more than 30 mmol/(m^2·day), i.e., 9.2 g/(m^2·week). Our study
404 suggests the sea-air flux during the strongest period in a year, i.e., February, could be much
405 larger. The average flux obtained here, 18.84 g/(m^2·week), is twice of the averaged value over a
406 longer period (November to February) reported/estimated by Gibsonab et al. (1999).
407 As the strongest surface unsaturation in summer, the Shelf region has a potential carbon
408 uptake of 8.10 Tg C for February, which accounts for approximately 4.05‰-5.4‰ of the net
409 global ocean CO_2 uptake according to Takahashi et al. (2009) while its total area is only $78*10^3$
410 km^2. Due to the constraint of sill, there is limited exchange between water masses in and outside
411 Prydz Bay. During winter, the dense water formed by brine ejection in the Bay, potentially
412 uptakes more anthropogenic CO_2 from the atmosphere, and descends to depth, enhancing the
413 acidification in the deep water. According to Shadwick et al. (2013), winter values of *p*H and Ω
414 decreased more remarkably than summer values. As the bottom water in Prydz Bay is a possible
415 source of Antarctic Bottom Water (Yabuki et al., 2006), the Shelf region may act as to transfer
416 anthropogenic CO_2 at the surface to the deep water, and then may influence the deep ocean
417 acidification in the long run.

The total carbon uptake in Prydz Bay of three regions integrated over the whole February 2015 was 18.7 TgC. The uncertainty depended on the errors for the wind speed, the scaling factor and the accuracy of SOM derived pCO_2 according to Eq.2. The scaling factor will yield a 20% uncertainty to regional flux estimation. The errors in wind speeds of Ascat dataset is assumed to be 6% (Xu et al., 2016) and will be 12% in quadratic wind speed. For the SOM derived pCO_2 the RMSE is 22.14 μatm. Considering the errors above and an uncertainty occurred when the sea-air computation expression was simplified (1.39%, Xu et al., 2016), the total uncertainty of the final uptake is ±4.93 TgC.

4 Summary

According to different controls factors of ocean pCO_2, the Prydz Bay region was divided into three sectors for February 2015. In Shelf region biological factor was the main control for oceanic pCO_2 while in Open-ocean region mixing and upwelling became the main controls. In Sea-ice region, due to the rapid sea ice changing, oceanic pCO_2 was controlled by both the biological and physical processes. SOM is an important tool to do the quantitative assessment of oceanic pCO_2 and succedent sea-air carbon flux especially in dynamic, high latitude, seasonally ice-covered region. The estimated results revealed that the SOM technique could reconstruct the variations of oceanic pCO_2 associated with bio-geochemical processes expressed by the variabilities in four proxy parameters: SST, CHL, MLD and SSS. The RMSE of the SOM derived oceanic pCO_2 is 22.14 μatm for the SOCAT dataset. Over February 2015, Prydz Bay region was a strong carbon sink with a carbon uptake of 18.7±4.93 TgC. Strong potential uptake of anthropogenic CO_2 in the Shelf region will enhance the acidification in the deep water of Prydz bay and then may influence the deep ocean acidification in the long run since it contributes to the formation of Antarctic bottom water.

Acknowledgments

This work is supported by National Natural Science Foundation of China (NSFC41506209, 41630969, 41476172, 41230529), Qingdao National Laboratory for marine science and technology (QNLM2016ORP0109), Chinese Projects for Investigations and Assessments of the Arctic and Antarctic (CHINARE2012-2020 for 01-04, 02-01, and 03-04). This work is also supported by Korea Polar Research Institute grants PE18060 and PE18070. We would like to

thank China Scholarship Council (201704180019) and State Administration of Foreign Experts Affairs P. R. China for their support in this research. We would like to thank the carbon group in GCMAC and the crew on R/V Xuelong for their support on the cruise. We are thankful to contributors of the SOCAT database and Mercator Ocean for providing the Global Forecast model output. We deeply appreciate Dr. Xianmin Hu in Bedford Institute of Oceanography, who provided us with useful technical instructions.

References

1. Bakker, D. C. E., Pfeil, B. Landa, C. S., Metzl, N., O'Brien, K. M., Olsen, A.,Smith, K., Cosca, C., Harasawa, S., Jones, S. D., Nakaoka, S., Nojiri, Y., Schuster, U., Steinhoff, T., Sweeney, C., Takahashi, T., Tilbrook, B., Wada, C., Wanninkhof, R., Alin, S. R., Balestrini, C. F., Barbero, L., Bates, N. R., Bianchi, A. A., Bonou, F., Boutin, J.,Bozec, Y., Burger, E. F., Cai, W.-J., Castle, R. D., Chen, L., Chierici, M., Currie, K., Evans, W., Featherstone, C., Feely, R. A., Fransson, A., Goyet, C., Greenwood, N., Gregor, L., Hankin, S., Hardman-Mountford, N. J., Harlay, J., Hauck, J., Hoppema, M., Humphreys, M. P., Hunt, C. W., Huss, B., Ibánhez, J. S. P., Johannessen, T., Keeling, R., Kitidis, V., Körtzinger, A., Kozyr, A., Krasakopoulou, E., Kuwata, A., Landschützer, 3P., Lauvset, S. K., Lefèvre, N., Lo Monaco, C., Manke, A., Mathis, J. T., Merlivat, L., Millero, F. J., Monteiro, P. M. S., Munro, D. R., Murata, A., Newberger, T., Omar, A. M., Ono, T., Paterson,K., Pearce, D., Pierrot, D., Robbins, L. L., Saito, S., Salisbury, J., Schlitzer, R., Schneider, B., Schweitzer, R., Sieger, R., Skjelvan, I., Sullivan, K. F., Sutherland, S. C., Sutton, A. J., Tadokoro, K., Telszewski, M., Tuma, M., Van Heuven, S. M. A. C., Vandemark, D., Ward, B., Watson, A. J., Xu, S.: A multi-decade record of high quality fCO_2 data in version 3 of the Surface Ocean CO_2 Atlas (SOCAT). Earth System Science Data 8: 383-413.doi:10.5194/essd-8-383-2016, 2016.

2. Brainerd, K. E., and Gregg, M. C.: Surface mixed and mixing layer depth, Deep Sea Res., part A, 42, 1521-1543, 1995.

3. Burkill, P. H., Edwards, E. S., Sleight, M. A.: Microzooplankton and their role in controlling phytoplankton growth in the marginal ice zone of the Bellingshausen Sea, Deep Sea Research Part II: Topical Studies in Oceanography, 42(4), 1277-1290, 1995.

4. Chen, L., Xu, S., Gao, Z., Chen, H., Zhang, Y., Zhan, J., Li, W.: Estimation of monthly air-sea CO_2 flux in the southern Atlantic and Indian Ocean using in-situ and remotely sensed data, Remote Sensing of Environment, 115(8), 1935-1941, 2011.

5. Dandonneau, Y.: Sea-surface partial pressure of carbon dioxide in the eastern equatorial Pacific (August 1991 to October 1992): A multivariate analysis of physical and biological factors, Deep Sea Research II, 42(2-3), 349-364, 1995.

6. Dong, S., Sprintall, J., Gille, S. T., Talley, L.: Southern Ocean mixed-layer depth from Argo float profiles, Journal of Geophysical Research, 113, C06013, doi: 10.1029/2006JC004051, 2008.

7. Edwards, A. M., Platt, T., Sathyendranath, S.: The high-nutrient, low-chlorophyll regime of the ocean: limits on biomass and nitrate before and after iron enrichment, Ecological Modelling, 171, 103-125, 2004.

8. Friedrich, T., Oschlies, A.: Neural network-based estimates of North Atlantic surface pCO_2 from satellite data: A methodological study, J. Geophys. Res., 114, C03020, doi:10.1029/2007JC004646, 2009a.

9. Friedrich, T., Oschlies, A.: Basin-scale pCO_2 maps estimated from ARGO float data: A model study, J. Geophys. Res., 114, C10012, doi:10.1029/2009JC005322, 2009b.

10. Gao, Z., Chen, L., Gao, Y.: Air-sea carbon fluxes and there controlling factors in the Prydz Bay in the Antarctic, Acta Oceanologica Sinica, 3(27), 136-146, 2008.

11. Gibsonab, J. A.E., Trullb, T. W.: Annual cycle of fCO_2 under sea-ice and in open water in Prydz Bay, east Antarctica, Marine Chemistry, Volume 66, Issues 3-4, 187-200, 1999.

12. Gibson, P. B., Perkins-Kirkpatrick, S. E., Uotila, P., Pepler, A. S., Alexander, L. V.: On the use of self-organizing maps for studying climate extremes, Journal of Geophysical Research: Atmospheres, 122, 3891-3903, 2017.

13. Hales, B., Strutton, P., Saraceno, M., Letelier, R., Takahashi, T., Feely, R., Sabine, C., Chavez, F.: Satellite-based prediction of pCO_2 in coastal waters of the eastern North Pacific, Progress in Oceanography, 103, 1-15, 2012.

14. Heil, P., I. Allison and V. I. Lytle: Seasonal and interannual variations of the oceanic heat flux under a landfast Antarctic sea ice cover, J. Geophys. Res., 101(C11), 25,741-25,752, doi: 10.1029/96JC01921, 1996.

15. Huang, J., Xu, F., Zhou, K., Xiu, P., Lin, Y.: Temporal evolution of near-surface chlorophyll over cyclonic eddy lifecycles in the southeastern Pacific, Journal of Geophysical Research: Oceans 122, 6165-6179, 2017a.

16. Huang, W., Chen, R., Yang, Z., Wang, B., Ma, W.: Exploring the combined effects of the

510 Arctic Oscillation and ENSO on the wintertime climate over East Asia using self-organizing
511 maps, Journal of Geophysical Research: Atmospheres, 122, 9107-9129, 2017b.
512 17. Iskandar, I.: Seasonal and interannual patterns of sea surface temperature in Banda Sea as
513 revealed by self-organizing map, Continental Shelf Research, 30, 1136-1148, 2010.
514 18. Jiang, L. Q., Cai, W. J., Wanninkhof, R., Wang, Y., Lüger, H.: Air–sea CO_2 fluxes on the U.S.
515 South Atlantic Bight: Spatial and seasonal variability, Journal of Geophysical Research, 113
516 (2008), C07019, doi:10.1029/2007JC004366, 2008.
517 19. Jo, Y. H., Dai, M. H., Zhai, W. D., Yan, X. H., Shang, S. L.: On the variations of sea surface
518 pCO_2 in the northern South China sea: A remote sensing based neural network approach,
519 Journal of Geophysical Research, 117, C08022, doi:10.1029/2011JC007745, 2012.
520 20. Kohonen, T.: Self-Organization and Associative Memory, Springer, Berlin, 1984.
521 21. Lafevre, N., Watson, A. J., Watson, A. R.: A comparison of multiple regression and neural
522 network techniques for mapping in situ pCO_2 data, Tellus B, 57(5), 375-384, 2005.
523 22. Laruelle, G. G., Landschützer, P., Gruber, N., Tison, J. L., Delille, B., Regnier, P.: Global
524 high resolution monthly pCO_2 climatology for the coastal ocean derived from neural
525 network interpolation, Biogeosciences, 14, 4545-4561, 2017.
526 23. Lei, R., Li, Z., Cheng, B., Zhang, Z., Heil, P.: Annual cycle of landfast sea ice in Prydz Bay,
527 East Antarctica, Journal of Geophysical Research Atmospheres, 115(C2), C02006,
528 doi:10.1029/2008JC005223, 2010.
529 24. Liu C., Wang Z., Cheng C., Xia R., Li B., Xie Z.: Modeling modified circumpolar deep
530 water intrusions onto the Prydz Bay continental shelf, East Antarctica, Journal of
531 Geophysical Research, Vol. 122, Issue 7, 5198-5217. DOI: 10.1002/2016JC012336, 2017.
532 25. Liu, Y., Weisberg, R. H., He, R.: Sea Surface Temperature Patterns on the West Florida Shelf
533 Using Growing Hierarchical Self-Organizing Maps, Journal of Atmospheric and Oceanic
534 Technology, 23, 325-338, 2006.
535 26. Lüger, H., Wallace, D. W. R., Körtzinger, A., Nojiri, Y.: The pCO_2 variability in the
536 midlatitude North Atlantic Ocean during a full annual cycle, Global Biogeochem. Cycles,
537 18, GB3023, doi:10.1029/2003GB002200, 2004.
538 27. Metzl, N., Brunet, C., Jabaud-Jan, A., Poisson, A., and Schauer, B.: Sumer and winter air-sea
539 CO_2 fluxes in the Southern Ocean, Deep-Sea Research, I53: 1548-1563, 2006.
540 28. Middleton, J. H., Humphries, S. E.: Thermohaline structure and mixing in the region of

Prydz Bay, Antarctica, Deep Sea Research Part A, Oceanographic Research Papers, 36(8), 1255-1266, 1989.

29. Morrison, J. M., Gaurin, S., Codispoti, L. A., Takahashi, T., Millero, F. J., Gardner, W. D., and Richardson, M. J.: Seasonal evolution of hydrographic properties in the Antarctic circumpolar current at 170W during 1997-1998, Deep-Sea Research, I48: 3943-3972, 2001.

30. Nakaoka, S., Telszewski, M., Nojiri, Y., Yasunaka, S., Miyazaki, C., Mukai, H., Usui, N.: Estimating temporal and spatial variation of ocean surface pCO_2 in the North Pacific using a self-organizing map neural network technique, Biogeosciences, 10, 6093-6106, 2013.

31. Nunes Vaz, R. A., Lennon, G. W.: Physical oceanography of the Prydz Bay region of Antarctic waters, Deep Sea Research Part I: Oceanography Research Papers, 43(5), 603-641, 1996.

32. Pfeil, B., Olsen, A., Bakker, D. C. E., Hankin, S., Koyuk, H., Kozyr, A., Malczyk, J., Manke, A., Metzl, N., Sabine, C. L., Akl, J., Alin, S. R., Bellerby, R. G. J., Borges, A., Boutin, J., Brown, P. J., Cai, W.-J., Chavez, F. P., Chen, A., Cosca, C., Fassbender, A. J., Feely, R. A., González-Dávila, M., Goyet, C., Hardman- Mountford, N., Heinze, C., Hood, M., Hoppema, M., Hunt, C. W., Hydes, D., Ishii, M., Johannessen, T., Jones, S. D., Key, R. M., Körtzinger, A., Landschützer, P., Lauvset, S. K., Lefèvre, N., Lenton, A., Lourantou, A., Merlivat, L., idorikawa, T., Mintrop, L., Miyazaki, C., Murata ,A., Nakadate, A., Nakano, Y., Nakaoka, Y. Nojiri, A. M. Omar, X. A. Padin, G.-H. Park, K. Paterson, F. F. Perez, S., Pierrot, D., Poisson, A., Ríos, A. F., Salisbury, J., Santana-Casiano, J. M., Sarma, V. V. S. S., Schlitzer, R., Schneider, B., Schuster, U., Sieger, R., Skjelvan, I., Steinhoff, T., Suzuki, T., Takahashi, T., Tedesco, K., Telszewski, M., Thomas, H., Tilbrook, B., Tjiputra, J., Vandemark, D., Veness, T., Wanninkhof, R., Watson, A. J., Weiss, R., Wong, C. S., and Yoshikawa-Inoue, H.: A uniform, quality controlled Surface Ocean CO_2 Atlas (SOCAT), Earth Syst. Sci. Data, 5, 125-143, doi:10.5194/essd-5-125-2013, 2013.

33. Pierrot, D., Neill, C., Sullivan, L., Castle, R., Wanninkhof, R., Lüger, H., Johannessen, T., Olsen, A., Feely, R. A., Cosca, C. E.: Recommendations for autonomous underway pCO_2 measuring systems and data-reduction routines, Deep-Sea Research Part II, 56, 512-522, 2009.

34. Rangama, Y., Boutin, J., Etcheto, J., Merlivat, L., Takahashi, T., Delille, B., Frankignoulle, M., Bakker, D. C. E.: Variability of the net air-sea CO_2 flux inferred from shipboard and

572 satellite measurements in the Southern Ocean south of Tasmania and New Zealand, Journal
573 of Geophysical Research: Oceans (1978-2012), 110(C9), doi: 10.1029/2004JC002619, 2005.
57435. Roden, N. P., Shadwick, E. H., Tilbrook, B., Trull, T. W.: Annual cycle of carbonate
575 chemistry and decadal change in coastal Prydz Bay, East Antarctica, Marine Chemistry,
576 155(4), 135-147, 2013.
57736. Rubin, S.I., Takahashi, T., Goddard, J.G.: Primary productivity and nutrient utilization ratios
578 in the Pacific sector of the Southern Ocean based on seasonal changes in seawater chemistry,
579 Deep-Sea Research I 45, 1211-1234, 1998.
58037. Sabine, L., Feely, R. A., Gruber, N., Key, R. M., Lee, K., Bullister, J. L., Wanninkhof, R.,
581 Wong, S., Wallace, D. W. R., Tilbrook, B., Millero, F. J., Peng, T.-H., Kozyr, A., Ono, T.,
582 and Rios, A. F.: The oceanic sink for anthropogenic CO_2, Science, 305, 367-371,
583 doi:10.1126/science.1097403, 2004.
58438. Sarma, V. V. S. S., Saino, T., Sasaoka, K., Nojiri, Y., Ono, T., Ishii, M., Inoue, H. Y.,
585 Matsumoto, K.: Basin-scale pCO_2 distribution using satellite sea surface temperature, Chl a,
586 and climatological salinity in the North Pacific in spring and summer, Global
587 Biogeochemical Cycles, 20, GB3005, doi:10.1029/2005GB002594, 2006.
58839. Shadwick, E. H., Trull, T. W., Thomas, H., Gibson, J. A. E.: Vulnerability of polar oceans to
589 anthropogenic acidification: comparison of Arctic and Antarctic seasonal cycles, Scientific
590 Reports, 3: 2339, doi: 10.1038/srep02339, 2013.
59140. Silulwane, N. F., Richardson, A. J., Shillington, F. A., Mitchell-Innes, B. A.: Identification
592 and classification of vertical chlorophyll patterns in the Benguela upwelling system and
593 Angola-Benguela front using an artificial neural network, South African Journal of Marine
594 Science, 23, 37-51, 2001.
59541. Smith, N. R., Zhaoqian, D., Kerry, K. R., Wright, S.: Water masses and circulation in the
596 region of Prydz Bay Antarctica, Deep-sea-research, 31, 1121-1147, 1984.
59742. Smith, N., Tréguer, P.: Physical and chemical oceanography in the vicinity of Prydz Bay,
598 Antarctica, Cambridge University Press, Cambridge, 1994.
59943. Spreen, G., Kaleschke, L., Heygster, G.: Sea ice remote sensing using AMSR-E 89 GHz
600 channels, J. Geophys. Res., 113, C02S03, doi:10.1029/2005JC003384, 2008.
60144. Sun, W. P., Han, Z. B., Hu, C. Y., Pan, J. M.: Particulate barium flux and its relationship with
602 export production on the continental shelf of Prydz Bay, east Antarctica, Marine Chemistry,

157, 86-92, 2013.

45. Sweeney, C., Hansell, D. A., Carlson, C. A., Codispoti, L. A., Gordon, L. I., Marra, J., Millero, F. J., Smith, W. O., Takahashi, T.: Biogeochemical regimes, net community production and carbon export in the Ross Sea, Antarctica, Deep Sea Research II, 47(15-16), 3369-3394, 2000.

46. Sweeney, C.: The annual cycle of surface water CO_2 and O_2 in the Ross Sea: a model for gas exchange on the continental shelves of Antarctic, Biogeochemistry of the Ross Sea, Antarctic Research Series, 78, 295-312, 2002.

47. Takahashi, T., Sutherland, S. C., Feely, R. A., and Wanninkhof, R.: Decadal change of the surface water pCO_2 in the North Pacific: A synthenesis of 35 years of observations, J. Geophys. Res., 111, C07S05, doi: 10.1029/2005JC003074, 2006.

48. Takahashi, T., Sweeney, C., Hales, B., Chipman, D. W., Newberger, T., Goddard, J. G., Iannuzzi, R. A., Sutherland, S. C.: The changing carbon cycle in the Southern Ocean, Oceanography, 25, 26-37, 2012.

49. Telszewski, M., Chazottes, A., Schuster, U., Watson, A. J., Moulin, C., Bakker, D. C. E., González-Dávila, M., Johannessen, T., Körtzinger, A., Lüger, H., Olsen, A., Omar, A., Padin, X. A., Ríos, A. F., Steinhoff, T., Santana-Casiano, M., Wallace, D. W. R., Wanninkhof, R.: Estimating the monthly pCO_2 distribution in the North Atlantic using a self-organizing neural network, Biogeoscience, 6, 1405-1421, 2009.

50. Thomson, R. E., and Fine, I. V.: Estimating mixed layer depth from oceanic profile data, J. Atmos. Oceanic Technol., 20, 319-329, 2003

51. Ultsch, A., Röske, F.: Self-organizing feature maps predicting sea levels, Information Sciences, 144, 91-125, 2002.

52. Vesanto, J.: Data Exploration Process Based on the Self-Organizing Map: the Finnish Academies of Technology, 2002.

53. Wanninkhof, R.: Relationship between wind speed and gas exchange over the ocean revisited, Limnology and Oceanography: Methods, 12, 351-362, 2014.

54. Wong, C. S., Christian, J. R., Emmy Wong, S. -K., Page, J., Xie, L., and Johannessen, S.: Carbon dioxide in surface seawater of the eastern North Pacific Ocean (Line P), 1973-2005, Deep-Sea Res., I, 57(5), 687-695, doi: 10.1016/j.dsr.2010.02.003, 2010.

55. Wu, L., Wang, R., Xiao, W., Ge, S., Chen, Z., Krijgsman, W.: Productivity-climate coupling

634 recorded in Pleistocene sediments off Prydz Bay (East Antarctica), Palaegeography,
635 Palaeoclimatology, Palaeoecology, 485, 260-270, 2017.
636 56. Xu, S., Chen, L., Chen, H., Li, J., Lin, W., Qi, D.: Sea-air CO_2 fluxes in the Southern Ocean
637 for the late spring and early summer in 2009, Remote Sensing of Environment, 175, 158-
638 166, 2016.
639 57. Yabuki, T., Suga, T., Hanawa, K., Matsuoka, K., Kiwada, H., and Watanabe, T.: Possible
640 source of the Antarctic Bottom Water in Prydz Bay region, J. Oceanogr., 62, 649-655, doi:
641 10.1007/s10872-006-0083-1, 2006.
642 58. Zeng, J., Nojiri, Y., Murphy, P. P., Wong, C. S., Fujinuma, Y.: A comparison of $\triangle pCO_2$
643 distributions in the northern North Pacific using results from a commercial vessel in 1995-
644 1999, Deep Sea Res., Part II, 49, 5303-5315, 2002.
645 59. Zeng, J. Nojiri, Y., Nakaoka, S., Nakajima, H., Shirai, T.: Surface ocean CO2 in 1990-2011
646 modelled using a feed-forward neural network, Geoscience Data Jounal, 2, 47-51, doi:
647 10.1002/gdj3.26, 2015.
648 60. Zeng, J., Mtsunaga, T., Saigusa, N., Shirai, T., Nakaoka, S., Tan, Z.: Technical note:
649 Evaluation of three machine learning models for surface ocean CO_2 mapping, Ocean Sci.,
650 13, 303-313, http://doi.org/10.5194/os-13-303-2017, 2017.
651